

Effect of Transducer Positioning in Active Noise Control

Sajil C. K., Biji C. L and Achuthsankar S. Nair

Abstract—Research in traditional Active Noise Control(ANC) often abstracts acoustic channels with band-limited filter coefficients. This is a limitation in exploring structural and positional aspects of ANC. As a solution to this, we propose the use of room acoustic models in ANC research. As a use case, we demonstrate anti-noise source position optimization using room acoustics models in achieving better noise control. Using numerical simulations, we show that level of cancellation can be improved up to 7.34 dB. All the codes and results are available in the Github repository <https://github.com/cksajil/ancram> in the spirit of reproducible research.

I. INTRODUCTION

Studies have proven that exposure to high sound pressure levels for extended periods of time can cause temporary or permanent hearing loss [1]. In the medical field, MRI scanners generate noise over 120 dB [2], which is often causing discomfort to the patients [3] as well as to doctors. There have been studies proving that the noise generated by fMRI scanners affect the scanning results also [4]. One solution to this is acoustic quiet zones generated by Active Noise Control(ANC), which have broad applications in medical, entertainment, automobiles [5], airplanes, recording studios etc [6]. Recently, noise cancellation concepts were found application in synthetic biology also [7].

Passive noise control uses bulky sound absorbent materials to mask unwanted sound, whose performance degrades for low-frequency sounds [6]. ANC systems use the principle of canceling the sound wave with its inverse or anti-noise. The idea made its first appearance in the patent of Paul Lueg [8]. Figure 1 shows a graphical description of a simple active noise control system. Compared to passive noise control techniques, ANC techniques are well able to control low as well as high-frequency noise components. Also, it does not require bulky materials, making it portable.

In the existing ANC literature, which has a history of 7 decades [9], the acoustic channels are mostly modeled using Finite Impulse Response(FIR) filters [10]. This approximation, used for ease of computation, limits researchers in studying the effects of physical aspects like transducer positioning, orientation, room reverberation, wall reflections, room structure etc. Positioning of transducers is an important parameter which is to be addressed in ANC [11]. Room Impulse Response(RIR) is analogous to an Impulse Response(IR) in Linear Time invariant(LTI) systems. The IR is considered to characterize the behavior of an LTI

This work was supported by University Grants Commission(UGC), New Delhi, India

Authors are with Department of Computational Biology and Bioinformatics, University of Kerala, Kerala, India
sajilckdb@keralauniversity.ac.in

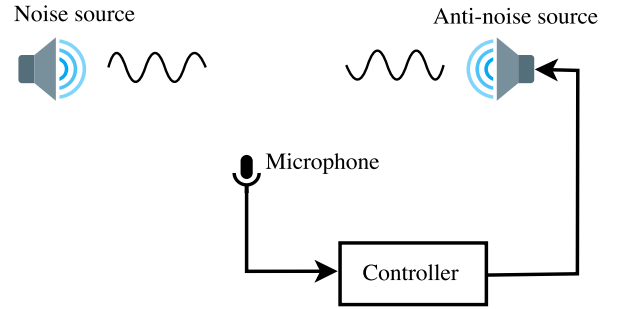


Fig. 1. Illustration of active noise control. The microphone receives the signal from the noise source and feeds into a controller. Controller analyses and drives the anti-noise source with phase inverted signal. Both signals cancel each other at the region of interest.

system completely. With room acoustics models, it is easy to calculate RIRs between any two points. Though some work make use of measured RIRs for simulation and experimental validation [12][13], a large scale utilization of RIRs using room acoustic models in ANC is still an unexplored area. In the subject area of room acoustics, simultaneous multi channel RIRs were used to reconstruct room geometry [14]. Inspired by their work, we focus to explore the use of RIRs in the Active Noise Cancellation(ANC) context. Our major contributions are:

- The use of room acoustic models in ANC.
- A new workflow model for ANC research.
- Optimization of anti-noise source location which improves cancellation up to 7.34 dB.

Section II introduces the fundamental of ANC concepts. Section III gives a brief overview of room acoustics models. The simulation details can be found in Section IV. Results are discussed in detail in Section V, including limitations of our approach and future scope. A tutorial style treatment of the research work is available at <https://cksajil.github.io/ancram/> aiming at a novice reader.

II. ANC PRELIMINARIES

Existing ANC systems use a controller to predict the noise of interest which is to be canceled. The ANC system picks up the noise using single or multiple microphones and passes on to the controller. The acoustic channel from the noise source to the zone of interest is represented using a primary propagation path $P(z)$. Similarly, the acoustic channel from anti-noise source to the zone of interest is represented using a secondary path $S(z)$. The adaptive filter keeps on updating its coefficients so that the error signal at the zone of interest is minimized. The weights of the controller filter

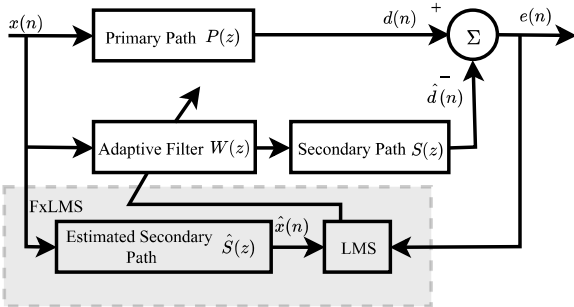


Fig. 2. Block diagram of FxLMS ANC System. $P(z)$ represent the acoustic channel from the noise source to the microphone. Similarly $S(z)$ represents the acoustic channel from anti-noise source to the microphone. The adaptive filter is controlled by the LMS algorithm which also considers the estimate of secondary path $\hat{S}(z)$ forming FxLMS.

are updated using adaptive filter algorithms like Least Mean Square(LMS), Recursive Least-Squares(RLS) or Filtered-x Least Mean Square (FxLMS).

Among the several types of ANC algorithms available, we tried our hypothesis with the popular and widely used FxLMS algorithm [15] due to its robustness and ease of computation. Figure 2 shows block diagram of a traditional FxLMS-ANC system. The transformation happening to source signal $x(n)$, after passing through the primary propagation path $P(z)$, is modeled using the following equation.

$$d(n) = x(n) * p(n) \quad (1)$$

The '*' here represents convolution operation. FxLMS algorithm also uses an estimate of the secondary path $\hat{S}(z)$, through which a filtered version of the source signal is calculated and passed on to the LMS filter.

$$\hat{x}(n) = \hat{s}(n) * x(n) \quad (2)$$

The error signal $e(n)$ and the filtered reference signal $\hat{x}(n)$ are used to update the adaptive filter weights.

$$w(n+1) = w(n) + \mu e(n) \hat{x}(n) \quad (3)$$

Here, $w(n) = [w_0(n) w_1(n) \dots w_{L-1}(n)]$ are the filter weights, L is the filter length and μ is the step size. In an ideal scenario, after several iteration, the predicted signal $\hat{d}(n)$ reaches inversely equal to $d(n)$ and $e(n)$ becomes zero. At this stage the filter weights $w(n)$ will be at its optimum converged range.

III. ROOM ACOUSTICS MODELS

Scientists working in acoustics or audio signal processing will often require a stage to test out and reproduce algorithms in specific acoustic scenarios. For this purpose, Room Acoustics Models(RAM) are often used, to recreate and reproduce room acoustics without any cross-model mismatch. Room acoustic models find its applications in beamforming [16],

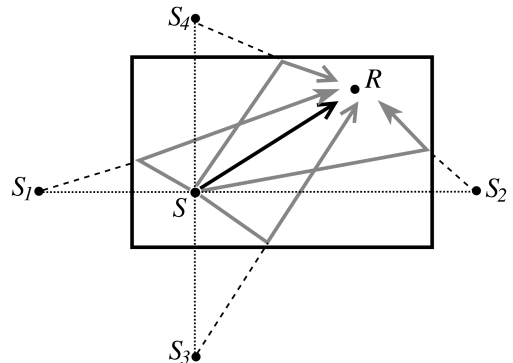


Fig. 3. Room impulse response as a superposition of direct sound and reflections. The direct sound (source S to receiver R) is shown with solid arrow and reflections with gray arrows. The reflections of the direct sound appear to the receiver as coming from imaginary sources S_1, S_2, S_3 and S_4 which are scaled and delayed accordingly.

acoustic auralisation, speech and audio processing [17], psychoacoustics studies etc [18].

A RIR model channel between a fixed source and a fixed receiver with direct path and reflections [14]. In RIR, apart from the direct sound, the receiver receives signals from different reflections. The acoustic energy gets attenuated after every reflection. A receiver at any point will be receiving direct sound superimposed with its reflections as reverberated sound. Image method [19] has been used widely to calculate RIRs for various room conditions. In image source model, the reflections are considered coming from virtual sources. Figure 3 shows a diagrammatic representation of RIR for an arbitrary 2D room.

IV. NUMERICAL SIMULATION SETUP

Figure 4 shows the flow diagram of the simulation. The room size was chosen arbitrarily to a size of $6 \times 4 \times 3$ meters. The z level of microphone, noise source and anti-noise source were fixed to a height of 1.53 for ease of computation. The x coordinate for noise source and microphone were chosen randomly from a uniform distribution within half-open interval $[1, 6)$. Similarly the y coordinate value for microphone and noise source were chosen randomly from a uniform distribution within half-open interval $[1, 4)$. The antinoise source positions were evenly spaced at a distance of 11 cm. For each position, anti-noise source is placed in that location and the primary path and secondary path, which are acoustic channels from the noise source to error microphone and anti-noise source to error microphone are calculated. The toolbox provided by Habets [20] have been used for generating the RIRs. These RIRs were passed onto the ANC simulation program. A total of 100 independent Monte-Carlo simulations were carried out for different noise source and microphone positions.

Table I shows an arbitrary case for illustration purpose. The noise source is fixed at center of room and the receiving microphone is placed arbitrarily at $(1, 3, 1.5)$ similar to [21]. Figure 5 shows energy decay curves of room impulse responses for the arbitrary case.

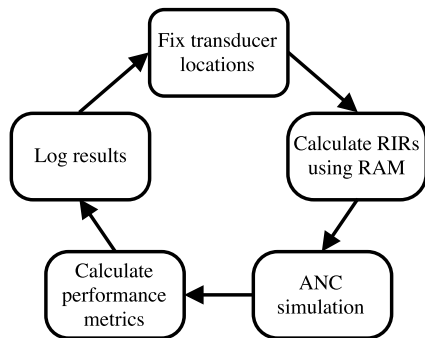


Fig. 4. Sequential steps in carrying out the simulation. For each anti-noise source location, RIRs were calculated using room acoustics models and passed onto ANC algorithm. The final canceled signal is analyzed and performance metrics (estimated attenuation and frequency specific attenuation) are logged for later reference.

TABLE I

SIMULATION SETTINGS USED FOR AN ARBITRARY CASE

No	Parameter	Value
1.	Room size	$6 \times 4 \times 3$ meters
2.	Noise source location	(3, 2, 1.5)
3.	Receiver location	(1, 3, 1.5)
4.	Reflection coefficients	[0.8, 0.7, 0.6, 0.5, 0.4, 0.5]

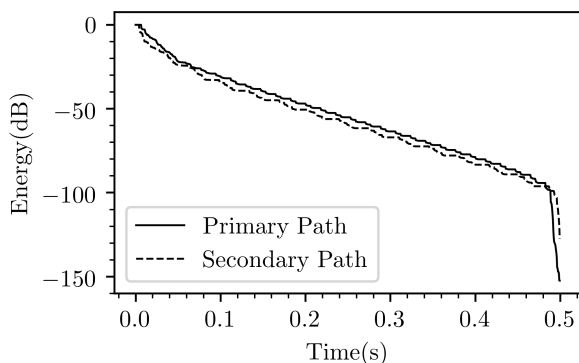


Fig. 5. Energy Decay Curves of Primary Path $P(z)$ and Secondary Path $S(z)$ for simulation parameters as per Table I

The source signal considered is sinusoidal with a wideband component. We used the same method to generate the source signal as used here [22] except the fact that we used open source scientific computing language Python [23] for signal generation and simulation. The method to generate the noise signal including source code can be found in the above reference. Similarly our source codes for the signal generation and simulation is available in the project GitHub repository [24]. The sinusoidal components consists of a fundamental frequency of 30 Hz and 2 other components which are multiples of the base frequency (i.e, 60 and 90 Hz). The signal is generated using Fourier synthesis method. The coefficients of sine components were, -1, -0.5 and 0.1 and that of cosine components were 2, 1 and 0.5. The Power Spectral Density (PSD) of the source signal is shown in Figure 6.

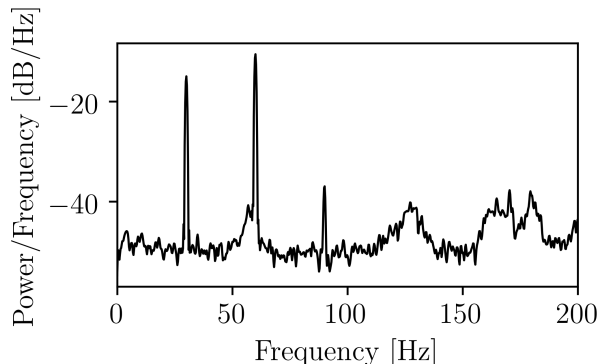


Fig. 6. Power Spectral Density of source signal used. The narrow band components can be seen at 30 Hz, 60 Hz and 90 Hz. A wide band component of variance 0.1 has been added to the signal.

TABLE II

PARAMETER VALUES USED FOR SIMULATION

No	Parameter	Value
1.	Sampling rate	2 kHz
2.	Room size	$6 \times 4 \times 3$ meters
3.	Simulation time	100 seconds
4.	Sound speed	343 meters/seconds
5.	Reverberation time	0.4 seconds
6.	RIR length	1000 samples
7.	Microphone type	omnidirectional

The sampling frequency (F_s) is fixed to 2 kHz according to Nyquist theorem. The adaptive filter length was fixed as 350 at $F_s = 2$ kHz, which is an important parameter determining ANC performance [25]. A step size of 1×10^{-5} was chosen since we wanted to focus on the level of cancellation achieved rather than how quickly it is achieved. Table II shows major settings and parameter values used for the simulation.

The assumptions made in this study are as follows. The room is considered to be rectangular in shape with size $6 \times 4 \times 3$ meters, without any furniture or moving objects. The reflection coefficient of the six walls are assigned equal and are considered to be frequency independent. The sources and receivers are assumed to be with omnidirectional. The algorithm was simulated for a simulation time of 100 seconds. The RIRs calculated were truncated to 1000 samples corresponding to its reverberation time (T_{60}). The secondary path transfer function which abstracts away reconstruction filter, power amplifier, loudspeaker, the acoustic channel from anti-noise source to receiver, pre-amplifier, anti-aliasing filter and Digital to Analog Converter (DAC) [26] is assumed to be known and identified in prior.

V. RESULTS AND DISCUSSION

The resulting signal is analyzed for determining the level of attenuation obtained. The performance measure used for analysis is, Estimated attenuation (A_{dB}), similar to [22], which is calculated using the following formula.

$$A_{dB} = 10 \log_{10} \frac{\text{Var}[d(n)]}{\text{Var}[e(n)]} \quad (4)$$

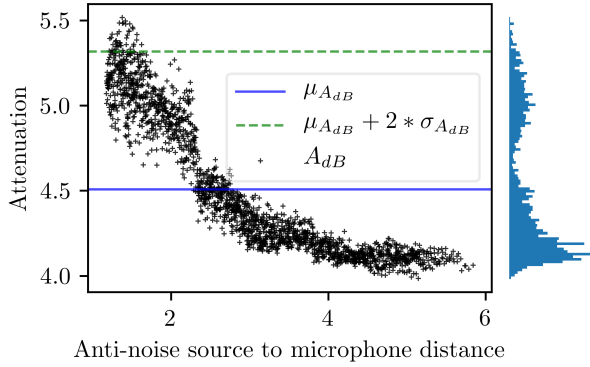


Fig. 7. Different A_{dB} levels obtained. The simulation settings were as per Table I. It can be seen that the distribution of attenuation levels shown on the right is bi-modal.

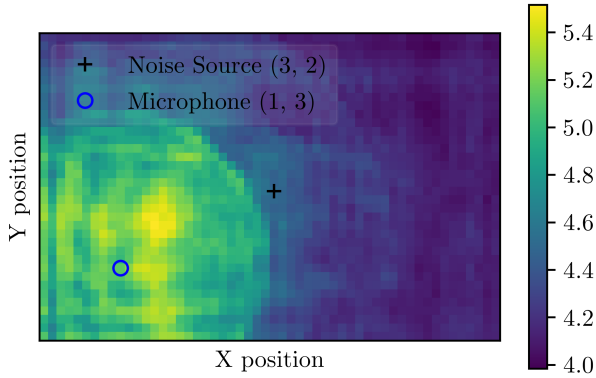


Fig. 8. Attenuation obtained with respect to each anti-noise source position. A region of locations with good attenuation can be seen around the microphone's location. The simulation settings were as per Table I

Where, $\text{Var}[\cdot]$ represents the mathematical operation of statistical variance. Since our signal of interest is of zero mean, this is equivalent to Mean Square Error(MSE) measure. We consider only the steady state value of error signal, $e(n)$ by trimming off the initial one-third of it. The parameter A_{dB} represents the overall attenuation of the noise signal which is calculated for each of the anti-noise source positions. Figure 7 shows different attenuation levels obtained for different anti-noise source positions as per simulation settings in Table I.

The attenuation levels can be visualized as a 2D image, where each point in the image will be representing the steady state attenuation for anti-noise source at that position. Figure 8 shows the attenuation levels corresponding to different anti-noise source positions as per simulation settings on Table I.

To determine good attenuation locations, we chose top 2.5 percentile attenuation levels by setting a threshold of $C = \mu_{A_{dB}} + 1.96 \times \sigma_{A_{dB}}$, where $\mu_{A_{dB}}$ and $\sigma_{A_{dB}}$ represents statistical mean and standard deviation of A_{dB} values. These attenuation values correspond to specific points in the room where the attenuation is relatively high. The corresponding binary figure is shown in the Figure 9.

As can be seen from the Figure 9, the best locations

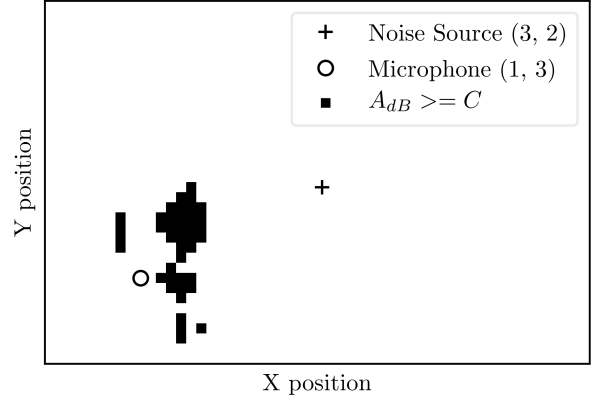


Fig. 9. Positions representing relatively good attenuation. It can be seen that the good anti-noise source positions are located near to error microphone. The simulation parameter values were as per Table I

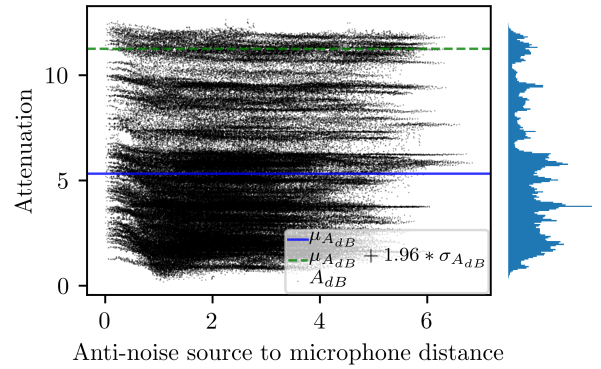


Fig. 10. Attenuation levels obtained for 100 Monte-Carlo simulations. It can be seen that the average attenuation is 5.31 dB and it can be optimized up to 12.65 dB making a difference of 7.34 dB.

fall near the error microphone location. We think this may due to spectral flatness of secondary path. When the anti-noise source gets closer to the receiver, the secondary path transfer function approaches flat frequency response and the cancellation improves. The attenuation levels of all cases are shown in the Figure 10. It can be seen that the attenuation levels spans in the range [0.17 dB, 12.65 dB] dB, with a mean attenuation of 5.32 dB and 3.02 dB standard deviation.

Figure 11 shows the Power Spectral Density(PSD) of the signal before and after cancellation at the optimum anti-noise source position. Our work differs from previous studies in the literature [27] where they concentrate on finding the optimum number of anti-noise sources. Also our results are similar to and reconfirms the findings shown here [26], where they optimize error microphone location by using spectral flatness of secondary path. Compared to these two studies, our method gives insight into best possible geometrical location for anti-noise source using room acoustic models.

The results show the possibility to optimize the anti-noise source location, provided the noise source and receiver positions are known and the RIRs or room reflections coefficients are available. This method has the potential to push further into better cancellation levels for ANC systems. In a realistic

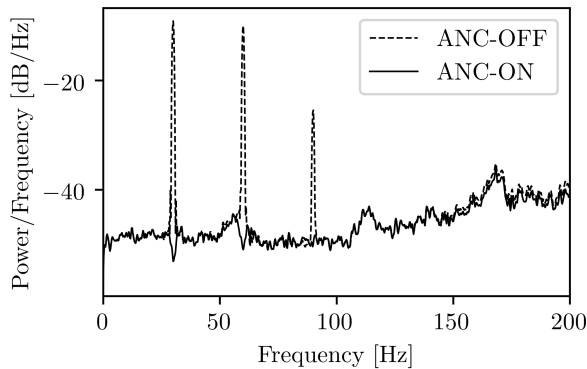


Fig. 11. Power Spectral Density of $d(n)$ and $e(n)$. It can be seen from the graph that the individual narrow band components are significantly attenuated after the the FxLMS algorithm converges to its stable performance.

scenario, it is possible to calculate reflection coefficients from readily available charts of sound absorption. Also, it is possible to calculate reflection coefficients from RIRs [28]. In most cases, room dimensions and shapes are available from blueprints or architecture design diagrams. This opens up the possibility to optimize transducer locations according to any user requirement scenario.

The major drawbacks to our approach are, measurement of real RIRs are time-consuming and tedious. We have not considered time varying changes of the acoustic channels. Also the dynamic variation of the error levels, i.e., how quickly the ANC system attenuates noise have also been not studied. We rather focused on the stable attenuation levels. The secondary path, which is a very important component in ANC systems is assumed to be known and identified. More accurate RIR models will require lengthy RIRs which contributes to computational complexity. There is a tremendous scope for improvement in our work including verifying the results in real lab conditions, improving ease of computation using a more concise representation of RIRs, moving observer or source scenario etc.

VI. CONCLUSION

We have investigated the possibility of using Room Acoustics Models in ANC scenario. We particularly focused on optimizing anti-noise source location once the noise source and receiver are fixed. Results prove that optimizing anti-noise source location improves the level of cancellation by approximately 7.34 dB. This opens up the possibility of optimizing several other physical parameters including, transducer orientation, room shape, etc., in achieving better noise control. Our results show that room acoustic models are good simulation tool which needs more attention by the ANC community.

VII. ACKNOWLEDGMENT

We are grateful to University Grants Commission(UGC), New Delhi, India for providing necessary funds to do this research, We are grateful to Campus Computing Facility(CCF)

and Department of Computational Biology and Bioinformatics, University of Kerala, India for extending the necessary facilities to carry out this research work.

REFERENCES

- [1] C. V. R. Sierra, M. J. Versluis, J. M. Hoogduin, and H. Duifhuis, "Acoustic fmri noise: linear time-invariant system model," *IEEE Transactions on Biomedical Engineering*, vol. 55, no. 9, pp. 2115–2123, 2008.
- [2] M. E. Ravicz, J. R. Melcher, and N. Y.-S. Kiang, "Acoustic noise during functional magnetic resonance imaging," *The Journal of the Acoustical Society of America*, vol. 108, no. 4, pp. 1683–1696, 2000.
- [3] G. Kannan, A. A. Milani, I. M. Panahi, and R. W. Briggs, "An efficient feedback active noise control algorithm based on reduced-order linear predictive modeling of fmri acoustic noise," *IEEE transactions on Biomedical Engineering*, vol. 58, no. 12, pp. 3303–3309, 2011.
- [4] S. Skouras, M. Gray, H. Critchley, and S. Koelsch, "fmri scanner noise interaction with affective neural processes," *PloS one*, vol. 8, no. 11, p. e80564, 2013.
- [5] P. N. Samarasinghe, W. Zhang, and T. D. Abhayapala, "Recent advances in active noise control inside automobile cabins: Toward quieter cars," *IEEE Signal Processing Magazine*, vol. 33, no. 6, pp. 61–73, 2016.
- [6] S. M. Kuo and D. R. Morgan, "Active noise control: a tutorial review," *Proceedings of the IEEE*, vol. 87, no. 6, pp. 943–973, 1999.
- [7] C. Zechner, G. Seelig, M. Rullan, and M. Khammash, "Molecular circuits for dynamic noise filtering," *Proceedings of the National Academy of Sciences*, vol. 113, no. 17, pp. 4729–4734, 2016.
- [8] L. Paul, "Process of silencing sound oscillations," 1936, uS Patent 2,043,416. [Online]. Available: <https://www.google.com/patents/US2043416>
- [9] N. V. George and G. Panda, "Advances in active noise control: A survey, with emphasis on recent nonlinear techniques," *Signal processing*, vol. 93, no. 2, pp. 363–377, 2013.
- [10] D. Veeravasantarao, S. Ajay, L. Behera *et al.*, "Adaptive active noise control schemes for headset applications," *IFAC Proceedings Volumes*, vol. 41, no. 2, pp. 7550–7555, 2008.
- [11] Y. Kajikawa, W.-S. Gan, and S. M. Kuo, "Recent advances on active noise control: open issues and innovative applications," *APSIPA Transactions on Signal and Information Processing*, vol. 1, 2012.
- [12] R. M. Reddy, I. M. Panahi, and R. Briggs, "Hybrid fxrls-fxnllms adaptive algorithm for active noise control in fmri application," *IEEE Transactions on Control Systems Technology*, vol. 19, no. 2, pp. 474–480, 2011.
- [13] I. T. Ardekani, J. P. Kaipio, A. Nasiri, H. Sharifzadeh, and W. H. Abdulla, "A statistical inverse problem approach to online secondary path modeling in active noise control," *IEEE/ACM Transactions on Audio, Speech, and Language Processing*, vol. 24, no. 1, pp. 54–64, 2016.
- [14] I. Dokmanić, R. Parhizkar, A. Walther, Y. M. Lu, and M. Vetterli, "Acoustic echoes reveal room shape," *Proceedings of the National Academy of Sciences*, vol. 110, no. 30, pp. 12 186–12 191, 2013.
- [15] D. Morgan, "An analysis of multiple correlation cancellation loops with a filter in the auxiliary path," *IEEE Transactions on Acoustics, Speech, and Signal Processing*, vol. 28, no. 4, pp. 454–467, 1980.
- [16] I. Dokmanić, R. Scheibler, and M. Vetterli, "Raking the cocktail party," *IEEE Journal of Selected Topics in Signal Processing*, vol. 9, no. 5, pp. 825–836, 2015.
- [17] E. De Sena, N. Antonello, M. Moonen, and T. Van Waterschoot, "On the modeling of rectangular geometries in room acoustic simulations," *IEEE Transactions on Audio, Speech, and Language Processing*, vol. 23, no. 4, pp. 774–786, 2015.
- [18] A. Wabnitz, N. Epain, C. Jin, and A. Van Schaik, "Room acoustics simulation for multichannel microphone arrays," in *Proceedings of the International Symposium on Room Acoustics*, 2010, pp. 1–6.
- [19] J. B. Allen and D. A. Berkley, "Image method for efficiently simulating small-room acoustics," *The Journal of the Acoustical Society of America*, vol. 65, no. 4, pp. 943–950, 1979.
- [20] E. A. Habets, "Room impulse response generator," *Technische Universiteit Eindhoven, Tech. Rep.*, vol. 2, no. 2.4, p. 1, 2006.
- [21] A. Barkefors, M. Sternad, and L.-J. Brännmark, "Design and analysis of linear quadratic gaussian feedforward controllers for active noise control," *IEEE/ACM Transactions on Audio, Speech and Language Processing (TASLP)*, vol. 22, no. 12, pp. 1777–1791, 2014.

- [22] D. Bismor, "Comments on a new feedforward hybrid anc system," *IEEE Signal Processing Letters*, vol. 21, no. 5, pp. 635–637, 2014.
- [23] T. E. Oliphant, "Python for scientific computing," *Computing in Science Engineering*, vol. 9, no. 3, pp. 10–20, May 2007.
- [24] C. K. Sajil. (2017) ancram. [Online]. Available: <https://github.com/cksajil/ancram>
- [25] D.-C. Chang and F.-T. Chu, "Feedforward active noise control with a new variable tap-length and step-size filtered-x lms algorithm," *IEEE/ACM transactions on audio, speech, and language processing*, vol. 22, no. 2, pp. 542–555, 2014.
- [26] S. M. Kuo, S. Mitra, and W.-S. Gan, "Active noise control system for headphone applications," *IEEE Transactions on Control Systems Technology*, vol. 14, no. 2, pp. 331–335, 2006.
- [27] S. K. Katsikas, D. Tsahalis, D. Manolas, and S. Xanthakis, "A genetic algorithm for active noise control actuator positioning," *Mechanical Systems and Signal Processing*, vol. 9, no. 6, pp. 697 – 705, 1995.
- [28] E. A. Lehmann and A. M. Johansson, "Prediction of energy decay in room impulse responses simulated with an image-source model," *The Journal of the Acoustical Society of America*, vol. 124, no. 1, pp. 269–277, 2008.